Analytical derivation of performance bounds of autonomous emergency brake systems

Jan Erik Stellet[1], Patrick Vogt[2], Jan Schumacher[1], Wolfgang Branz[1], J. Marius Zöllner[3]

***Abstract*— Autonomous emergency brake (AEB) systems have to decide on brake interventions based on an uncertain and incomplete perception of the environment. This paper analyses theoretical limitations in AEB systems caused by noisy sensor measurements and uncertain prediction models. Such performance bounds can be used to derive sensor accuracy constraints, to identify challenging scenarios or to develop objective metrics.**

In contrast to most previous studies, this work focusses on analytical derivations. To this end, the Cramér-Rao bound of the best attainable state estimation covariance is derived from a model of sensor measurement errors. This state- and time-dependent covariance is then propagated to an AEB decision making logic that is based on a criticality measure. Additional inherent prediction uncertainty in this risk assessment is taken into account. The effectiveness of the AEB subject to uncertainties is compared to the deterministic baseline case in terms of the brake activation time and the collision energy reduction.

I. Introduction

Autonomous emergency brake systems employ surround environment perception in order to detect critical driving situations and to perform an emergency brake intervention, if necessary. Fig. 1 depicts a typical use case. On a high level of abstraction, an AEB system is described by the concatenation of an environment sensor for perceiving obstacles, a tracking filter for estimating the motion state and a situation risk assessment logic for triggering a brake intervention. This signal processing chain is outlined in the upper part of Fig. 2.

However, due to measurement errors and an incomplete environment perception, the decision making is subject to uncertainties. This work addresses the question of how uncertainties affect the timely activation of a brake intervention and how this varies among different scenarios. In particular, upper, optimistic bounds are to be derived. Such a study can be useful for many purposes [1], e.g. the definition of requirements, sensitivity analyses or for adjusting the sensor and system parameters.

To this end, probabilistic models of uncertainty in an exemplary AEB signal processing are assumed as shown in the lower part of Fig. 2. The foundations of these models have been presented in the authors' previous works. The modelling approach considers uncertainties in stereo vision measurements [2], state estimates, vehicle trajectory predictions [3] and algorithms for risk assessment [4].

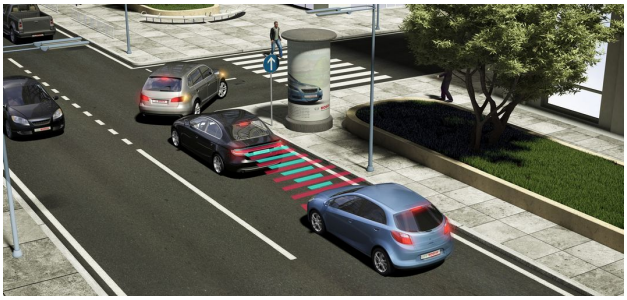

Fig. 1: Illustration of an AEB intervention scenario.

This paper entails the following **contributions**: First, a framework which integrates the aforementioned individual models is proposed in Sec. III-B. Second, explicit expressions for the collision energy reduction achievable by an AEB system are derived in Sec. IV-A. Third, an aggregate overall assessment is obtained in Sec. IV-C by weighting with empirical scenario parameter distributions.

The **outline** of this work is as follows: Differences and similarities to existing works are detailed in Sec. II. Subsequently, Sec. III introduces the representation of scenarios, the modelling of uncertainties in the AEB system and a metric to assess the difference between the ideal and uncertain case. Sec. IV presents numerical results for an exemplary parametrisation and discusses their implications. A summary in Sec. V concludes this work.

II. Related work

Previous related publications differ by the use of numerical or analytical methods for uncertainty propagation.

Numerical studies are presented in [5] for vehicle collision avoidance systems and pedestrian protection in [6], [7]. The latter works investigate the expected benefit of different evasive manoeuvres under uncertain future motion of the pedestrian. The probability and severity of the simulated accidents are used as evaluation metrics.

A drawback that is shared by these simulation-based approaches is that they rely on actual implementations of (sub-) optimal algorithms, e.g. state estimators. Thus, only numerical results that apply to a specific system can be obtained. More generic conclusions can be drawn with analytical models. By employing models of theoretical performance bounds, which apply to any implementation, fundamental limitations can be revealed.

[1]J. Stellet, J. Schumacher and W. Branz are with Robert Bosch GmbH, Corporate Research, Vehicle Safety and Assistance Systems, 71272 Renningen, Germany.

[2]P. Vogt is with the Department of Control Systems and Mechatronics (RTM), Technical University of Darmstadt, 64283 Darmstadt, Germany.

[3]J. Marius Zöllner is with Research Center for Information Technology (FZI), 76131 Karlsruhe, Germany.

 DOI 10.1109/IVS.2016.7535389

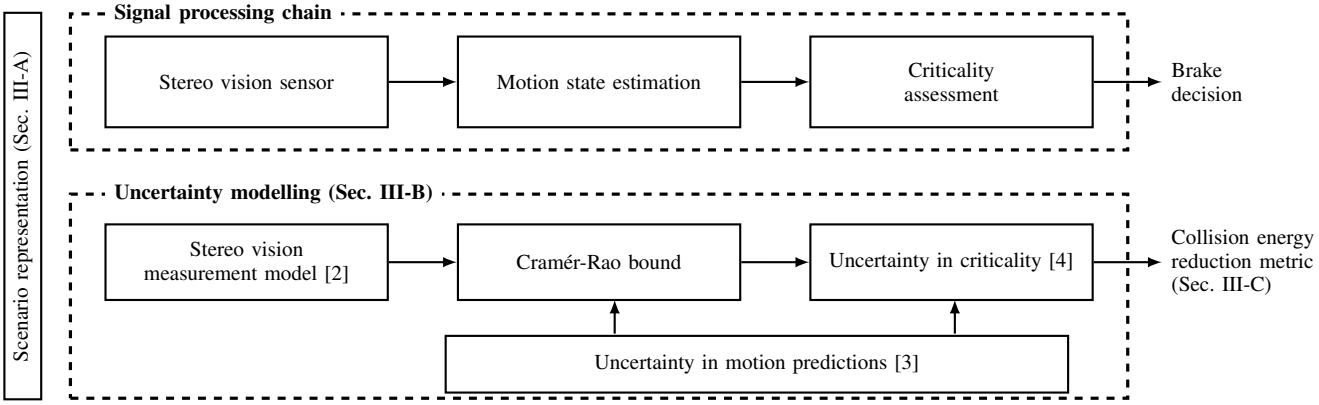

Fig. 2: Signal processing chain of AEB system (top) and overview on probabilistic models (below).

Recently, a remarkable, rigorous analytical derivation of performance bounds in AEB systems has been presented in [1]. Although a similar objective is pursued in this work, some distinct differences will lead to conceptually complementary results:

- Errors in the state estimates are modelled with constant upper bounds in [1], whereas a fully probabilistic model is used in this work. This time- and state-dependent model takes sensor-specific effects into account.
- Since only upper bounds on the errors are considered in [1], the worst case performance is derived. This work on the other hand studies the opposite case of optimistic lower bounds on the error covariances.
- The effectiveness of an AEB system is measured in terms of the activation timing in [1]. This work additionally considers the collision energy reduction as a metric with a clear physical interpretation.

III. Models, parametrisations and metric

This section describes the foundations of the analysis and comprises three parts. First, the considered scenarios are formalised in Sec. III-A. Second, the propagation of uncertainties in the signal processing chain from Fig. 2 is detailed in Sec. III-B. Finally, the impact of uncertainties on the AEB performance will be evaluated in terms of the collision energy reduction. This physically motivated metric is detailed in Sec. III-C.

A. Scenario representation

The primary type of accidents which are addressed by an AEB are collisions with a preceding vehicle. According to [8], these contribute to 30% of all accidents on German roads. In-depth analyses reveal the cause of approximately two thirds of these accidents being that the driver of a preceding vehicle is suddenly forced to brake strongly.

Therefore, rear-end accidents between the ego-vehicle and one preceding vehicle in longitudinal traffic are considered. In order to obtain more comprehensive results than only an evaluation for particular trajectories, a parametrisable model is introduced to describe entire families of trajectories.

Following the works [1], [5], the longitudinal relative motion between the two vehicles is modelled with piece-wise constant accelerations. The preceding vehicle's trajectories are modelled relative to the ego-vehicle which reduces the number of parameters that are needed to describe a scenario. These parameters are the initial distance $x_0 > 0$, the relative speed $v_{x,0} \leq 0$ and accelerations. It is assumed that the preceding vehicle brakes with a constant acceleration $a_x^{\mathrm{o}} \leq 0$ at time $t = 0$ as depicted in Fig. 1. An AEB brake intervention of the ego-vehicle starts at the time $t_{\mathrm{B}} \geq 0$ with a constant deceleration $a_x^{\mathrm{e}} \leq 0$. The relative motion is thus defined by a piece-wise constant acceleration $a_x(t)$:

$$a_x(t) = \begin{cases} a_x^{\mathrm{o}} & t < t_{\mathrm{B}} \\ a_x^{\mathrm{o}} - a_x^{\mathrm{e}} & t \geq t_{\mathrm{B}} \end{cases} . \tag{1}$$

The time evolution of the relative velocity $v_x(t)$ and distance $x(t)$ follows by integrating (1) with the initial values.

A potential inaccuracy of this model occurs if a vehicle has decelerated until standstill and remains fully stopped thereafter. This effect is concealed by considering solely the relative motion. In principle, all derivations can be performed in a similar manner as presented in the following but taking the additional special case of a standing vehicle into account. For conciseness, this is not elaborated here.

One way to visualise the parameter space of the scenarios is a phase portrait as shown in Fig. 3. Three cases that correspond to different values of a_x^{o} are depicted. An emergency brake intervention changes the direction of a trajectory. A collision is avoided if the trajectory does not cross the v_x-axis, which applies to all initial states in the green area of the phase plane. This subset of initial states is separated from scenarios where a collision is not entirely avoidable by the boundary

$$2x_0 \left(a_x^{\mathrm{o}} - a_x^{\mathrm{e}}\right) - v_{x,0}^2 = 0 . \tag{2}$$

These considerations suggest that the distribution of the initial states in real traffic situations has to be taken into account for a meaningful evaluation. Empirical weights are obtained from the following data sources:

- The initial relative motion state $(x_0, v_{x,0})$ is assumed to belong to normal car-following behaviour. Therefore,

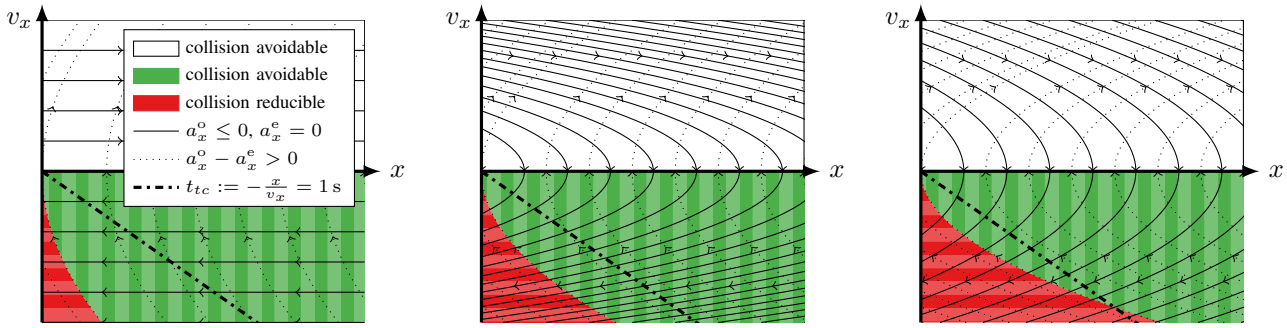

(a) $a_x^{\mathrm{o}} = 0\,\mathrm{m/s^2}$ (b) $a_x^{\mathrm{o}} = -2\,\mathrm{m/s^2}$ (c) $a_x^{\mathrm{o}} = -3\,\mathrm{m/s^2}$

Fig. 3: Trajectories and region of avoidable collisions for different object accelerations a_x^{o} in terms of distance x and relative velocity v_x. Solid lines show the trajectory prior to an emergency brake intervention and dotted lines with the emergency brake ($a_x^{\mathrm{e}} = -6\,\mathrm{m/s^2}$) applied. Green areas in the phase plane denote initial states for which a collision is still avoidable whereas its effect is only reducible in the red areas.

a dataset which comprises 170 h of raw recordings of vehicle trajectories is analysed. Further details on this dataset and its pre-processing are given in [3]. The resulting distribution is visualised in Fig. 4a.

- The acceleration a_x^{o} of the preceding vehicle, which eventually causes a collision, is retrieved from the German In-Depth Accident Study (GIDAS). It is not the scope of this work to perform a detailed simulation of each individual recorded accident, since they differ by a multitude of situation-specific factors. Instead, only the mean deceleration of the preceding vehicle prior to the collision is considered. Values for 111 relevant cases have been identified in [5] and are shown in Fig. 4b. We remark that only accidents with injuries are contained in the dataset. Collisions with minor damage are thus under-represented.

In conclusion, traffic scenarios with an impending rear-end collision are concisely parametrised by the initial distance and relative velocity as well as a constant deceleration of the preceding vehicle. Distributions of the state combinations are obtained from empirical data.

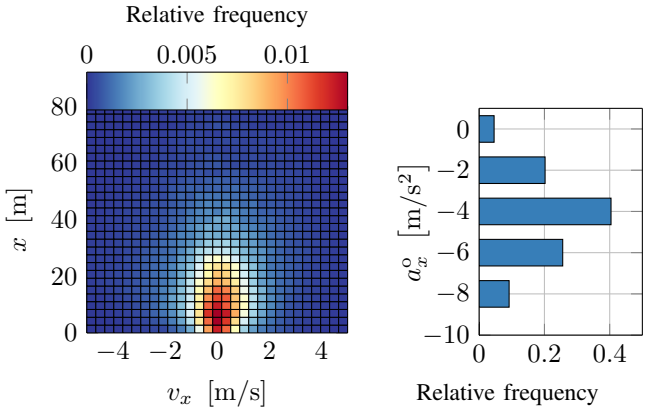

(a) Distance x and relative velocity v_x to leading vehicle in the same lane. (b) Mean acceleration of leading vehicle in rear-end collisions according to [5].

Fig. 4: Empirical distributions of scenario parameters: (a) Initial relative motion state $\mathbf{x}_0$, (b) Object acceleration a_x^{o}.

B. Modelling of uncertainty in an AEB system

This section details the AEB signal processing chain from Fig. 2 and the probabilistic modelling of uncertainties. First, a stereo vision sensor is assumed to measure the distance to a preceding vehicle. These measurements, which are obtained with a constant sampling time T_{s}, are affected by distance-dependent noise. Second, the propagation of the measurement uncertainty to the state estimates is modelled by the Cramér-Rao lower bound (CRB). This yields an optimistic approximation of the estimation error covariance of any practical filter. Third, a criticality measure termed the *brake-threat-number (BTN)* is employed for decision making. Under ideal conditions, this algorithm guarantees that a collision is avoided by the emergency brake intervention in the last possible moment. State estimation errors and uncertainty of motion predictions are propagated to a probabilistic model of this criticality measure.

Note that this analysis can be easily extended to other sensors, criticality measures or dynamical models. The specific examples shall illustrate typical effects, but most results will be derived in generic analytical form.

1) Stereo vision distance measurements: Measurements of the distance to a preceding vehicle are modelled in a stereo vision sensor's disparity coordinates d first and later transformed to Cartesian distances x.

We assume a model of a simplified object detection algorithm which aggregates a disparity image column-wise, as detailed in [2]. The measured disparity d that corresponds to the preceding vehicle is modelled as a Gaussian random variable $d \sim \mathcal{N}(\mu_d, \sigma_d^2)$. The variance σ_d^2 is inversely proportional to the number of image rows $n_{\Delta v,\mathrm{obj}}$ which the object covers in the image and over which the detection algorithm aggregates. This number can be calculated in dependence of the distance x and the object height h_{obj}. Disparity measurements $\bar{d}_i$ from individual rows $i = 1, \ldots, n_{\Delta v,\mathrm{obj}}$ are assumed to be affected by independent zero mean errors

with a variance of $\sigma_{\bar{d}}^2$. This leads to the variance σ_d^2 of the aggregate disparity measurement d:

$$\sigma_d^2 = \frac{1}{n_{\Delta v,\mathrm{obj}}}\sigma_{\bar{d}}^2 = \frac{x}{c_\mathrm{k} h_\mathrm{obj}}\sigma_{\bar{d}}^2 \,. \tag{3}$$

A linearisation-based transformation to a Cartesian distance $x \sim \mathcal{N}\big(\mu_x, \sigma_x^2\big)$ is given by [9]:

$$\mu_x = \frac{c_\mathrm{k} b_\mathrm{w}}{\mu_d} \,, \quad \sigma_x^2 = \left(\frac{c_\mathrm{k} b_\mathrm{w}}{\mu_d^2}\right)^2 \sigma_d^2 = \frac{\mu_x^4}{\left(c_\mathrm{k} b_\mathrm{w}\right)^2}\sigma_d^2 \,. \tag{4}$$

Here, c_k and b_w denote parameters of the camera. Note that the variance σ_x^2 is strongly distance-dependent.

2) Motion state estimates: The relative motion between the two vehicles is written as state vector $\mathbf{x} \coloneqq \left[\, x \;\, v_x \;\, a_x \,\right]^\top$ and assumed to follow a constant acceleration (CA) model with process noise power density S_x. The discrete time state transition is

$$\mathbf{x}_{k+1} = \begin{bmatrix} 1 & T_\mathrm{s} & \frac{1}{2}T_\mathrm{s}^2 \\ 0 & 1 & T_\mathrm{s} \\ 0 & 0 & 1 \end{bmatrix} \mathbf{x}_k + \mathbf{w}_k \,, \quad \mathbf{w}_k \sim \mathcal{N}\big(\mathbf{0}, \mathbf{Q}\big) \tag{5a}$$

with a sampling time T_s and

$$\mathbf{Q} = \begin{bmatrix} \frac{1}{20}T_\mathrm{s}^5 & \frac{1}{8}T_\mathrm{s}^4 & \frac{1}{6}T_\mathrm{s}^3 \\ \frac{1}{8}T_\mathrm{s}^4 & \frac{1}{3}T_\mathrm{s}^3 & \frac{1}{2}T_\mathrm{s}^2 \\ \frac{1}{6}T_\mathrm{s}^3 & \frac{1}{2}T_\mathrm{s}^2 & T_\mathrm{s} \end{bmatrix} S_x \,. \tag{5b}$$

A motion state estimate $\hat{\mathbf{x}}_k$ can be calculated for this system, e.g. with an extended Kalman filter. However, we will not focus on the implementation of such a filter but on the covariance $\mathbf{\Sigma}_{\hat{\mathbf{x}}_k} \coloneqq \mathrm{cov}\left(\hat{\mathbf{x}}_k - \mathbf{x}_k\right)$ of the state estimation error. The CRB $\mathcal{I}_{\mathbf{x}_k}^{-1} \preceq \mathbf{\Sigma}_{\hat{\mathbf{x}}_k}$ provides an optimistic lower bound for any unbiased estimator. This bound can be recursively calculated, see e.g. [10], [11].

Although the phase portrait in Fig. 3 suggests that trajectories which start at different initial states may eventually lie on the same trajectory, treating them in combined form is not possible. Using such a compact scenario description, based on subsets of all trajectories with a common end state, is proposed in [1]. Unfortunately, this is not applicable if effects that depend on the state history are taken into account. Since the CRB is in general time- and state-dependent, trajectories are considered individually for each triple of initial values $(x_0, v_{x,0}, a_x^\mathrm{o})$ in this work.

Attention has to be paid to the discrete-time nature of the system. The sampling time T_s determines how frequently new sensor measurements arrive at the state estimator. This in turn influences the accuracy of a state estimate $\mathbf{\Sigma}_{\hat{\mathbf{x}}_k}$, the uncertainty in the criticality measure and thus the time at which a brake intervention will be triggered.

However, it is out of the scope of this work to analyse the effects of unsynchronised sampling in general. Thus, a simplified approach is pursued: Firstly, the expected value of the state estimates are treated as continuous time variables $\hat{\mathbf{x}}_k \to \hat{\mathbf{x}}\,(t)$ which corresponds to $T_\mathrm{s} \to 0$. Secondly, the corresponding covariance matrix $\mathbf{\Sigma}_{\hat{\mathbf{x}}}\,(t) \coloneqq \mathcal{I}_{\mathbf{x}_{k^*}}^{-1}$ is calculated from the discrete time recursion until $k^* = \lceil \frac{t}{T_\mathrm{s}} - 1 \rceil$.

3) Criticality measures: As in [1], the *brake-threat-number (BTN)* is employed.[1] This criticality measure quantifies risk as the instantaneous brake deceleration of the ego-vehicle that is required to avoid an imminent collision. Given the motion state $\mathbf{x}$, the criticality $\kappa\,(\mathbf{x})$ is defined as [12]:

$$\kappa\,(\mathbf{x}) = a_x - \frac{v_x^2}{2x} \,. \tag{6}$$

Note that $\kappa\,(\mathbf{x})$ defines a deceleration and is thus negative. An AEB emergency brake intervention is triggered if

$$\kappa\big(\mathbf{x}\,(t)\big) \leq \kappa_0 \tag{7}$$

with a threshold value $\kappa_0 < 0$ that can be interpreted as the required deceleration for collision avoidance.

Uncertainty in this criticality estimate is modelled by a Gaussian distribution $\kappa\,(\mathbf{x}) \sim \mathcal{N}\big(\mu_\kappa, \sigma_\kappa^2\big)$. The variance σ_κ^2 can be calculated from the state estimate's covariance $\mathbf{\Sigma}_{\hat{\mathbf{x}}}$ and a model of the prediction errors. A CA motion model (5) is implicitly contained in (6) to predict the future relative vehicle motion. Prediction errors in such kinematic motion models have been analysed and approximated by Gaussian white process noise in [3]. The power spectral density S_x of the noise model has been estimated from recorded vehicle trajectories.

Propagating these uncertainties to the criticality measure according to the framework that has been proposed in [4] yields the following closed-form result:

$$\mu_\kappa = \kappa\,(\mathbf{x}) \;, \tag{8a}$$

$$\sigma_\kappa^2 = \big(\nabla_\mathbf{x}\kappa\,(\mathbf{x})\big) \cdot \mathbf{\Sigma}_{\hat{\mathbf{x}}} \cdot \big(\nabla_\mathbf{x}\kappa\,(\mathbf{x})\big)^\top - \frac{2x}{5v_x}S_x \,, \tag{8b}$$

$$\text{with} \quad \nabla_\mathbf{x}\kappa\,(\mathbf{x}) = \begin{bmatrix} \frac{v_x^2}{2x^2} & -\frac{v_x}{x} & 1 \end{bmatrix} \,. \tag{8c}$$

A Bayesian generalisation of the brake activation condition (7) to a system subject to known uncertainties reads

$$\mathrm{P}\big(\kappa\big(\mathbf{x}\,(t)\big) \leq \kappa_0\big) = \int_{-\infty}^{\kappa_0} \mathcal{N}\big(\kappa; \mu_\kappa\,(t)\,, \sigma_\kappa^2\,(t)\big)\mathrm{d}\kappa \geq 1 - \alpha \tag{9}$$

with a predefined confidence level $1 - \alpha$ [13].

For a given trajectory $\mathbf{x}\,(t)$, the deterministic criterion (7) can be solved for the time of intervention t_B. We will regard this value as baseline. Similarly, solving the Bayesian criterion (9) for t yields the braking time $t_{\mathrm{B},\mathfrak{U}}$ under consideration of uncertainties. The analysis in Sec. IV will focus on the difference between both cases.

C. Collision energy reduction metric

In order to assess the effectiveness of an AEB brake intervention, we follow the approach from [14] and evaluate the relative reduction of the collision energy. To this end, the kinetic impact energy $E_\mathrm{coll} = \frac{1}{2}mv_\mathrm{coll}^2$ of an inelastic collision with the relative collision velocity v_coll and vehicle

[1] Multiple criticality measures that correspond to different evasive actions in longitudinal and lateral direction are analysed in [1]. These measures are eventually combined by taking the minimum value. All findings of this work concern solely the longitudinal criticality but could be reiterated for additional measures.

TABLE I: Model parameter values of numerical example.

Variable	Value
Measurement model (3):	$c_{\mathrm{k}} b_{\mathrm{w}} = 121\,\mathrm{m}\cdot\mathrm{pel}\,, \quad \sigma_{\tilde{d}}^2 = (0.1\,\mathrm{pel})^2\,,$ $h_{\mathrm{obj}} = 1.5\,\mathrm{m}$
Initial state covariance:	$\boldsymbol{\Sigma}_{\hat{\mathbf{x}}_0} = \mathrm{diag}\left([\,100\,\mathrm{m}^2 \;\; 25\,\mathrm{m}^2/\mathrm{s}^2 \;\; 4\,\mathrm{m}^2/\mathrm{s}^4\,]\right)$
Sampling time:	$T_{\mathrm{s}} = 0.0675\,\mathrm{s}$
Process noise:	$S_x = 2\cdot 0.261\,\mathrm{m}^2/\mathrm{s}^6\mathrm{s}^{-1}$
Confidence level:	$1-\alpha = 90\%$
AEB brake deceleration:	$a_x^{\mathrm{e}} = -6\,\mathrm{m/s}^2$
BTN activation threshold:	$\kappa_0 = a_x^{\mathrm{e}} = -6\,\mathrm{m/s}^2$

mass m is calculated. A measure of effectiveness is then obtained from the difference between the case with ($E_{\mathrm{coll,B}}$) and without brake intervention (E_{coll}). After normalising this difference by E_{coll}, one obtains the dimensionless relative collision energy reduction $\Delta E \in [0,1]$:

$$\Delta E = \frac{E_{\mathrm{coll}} - E_{\mathrm{coll,B}}}{E_{\mathrm{coll}}} = 1 - \left(1 - \frac{v_{\mathrm{coll}} - v_{\mathrm{coll,B}}}{v_{\mathrm{coll}}}\right)^2 . \quad (10)$$

ΔE depends solely on the velocity at the time of collision. For the parametric trajectory model from Sec. III-A, closed-form expressions can be derived. Without brake intervention one obtains

$$v_{\mathrm{coll}} = v_{x,0} + a_x^{\mathrm{o}} t_{\mathrm{coll}} \quad (11a)$$

where t_{coll} denotes the time of collision. If an emergency brake manoeuvre with a deceleration $a_x^{\mathrm{e}} < 0$ is initiated at the time $0 \le t_{\mathrm{B}} \le t_{\mathrm{coll}}$, $v_{\mathrm{coll,B}}$ becomes a function of t_{B}:

$$v_{\mathrm{coll,B}} = v_{x,0} + a_x^{\mathrm{o}} t_{\mathrm{coll,B}} - a_x^{\mathrm{e}} \left(t_{\mathrm{coll,B}} - t_{\mathrm{B}}\right) . \quad (11b)$$

The collision times t_{coll} and $t_{\mathrm{coll,B}}$ are readily available and finally, a closed-form expression for ΔE depending on t_{B} can be derived. We leave out the details here but will provide more explicit results in the following section. To this end, t_{B} will be derived for the brake activation criteria (7) and (9).

IV. Effect of uncertainties on AEB brake interventions

This section uses the previously introduced models to assess the influence of uncertainties on the effectiveness of an AEB system. The analysis consists of three parts: First, the ideal baseline case without uncertainty is studied in Sec. IV-A. Second, uncertainties are taken into account in Sec. IV-B. Third, the results are aggregated with the empirical weights for the scenario parameters in Sec. IV-C.

Numerical results are derived for a specific exemplary system which is characterised by the parameter values given in Tab. I.

A. Ideal case without uncertainties

Firstly, the time of activation t_{B} is calculated for the BTN (6). Inserting the trajectory model (1) into the activation condition (7) and solving for t yields

$$t_{\mathrm{B}} = \begin{cases} 0, & \mathbf{x}_0 \in \mathcal{K} \\ \begin{cases} -\frac{x_0}{v_{x,0}} - \frac{v_{x,0}}{2\kappa_0}, & a_x^{\mathrm{o}} = 0 \\ -\frac{v_{x,0}}{a_x^{\mathrm{o}}} + \sqrt{\frac{v_{x,0}^2 - 2x_0 a_x^{\mathrm{o}}}{(a_x^{\mathrm{o}})^2}\,\frac{\kappa_0 - a_x^{\mathrm{o}}}{\kappa_0}}, & a_x^{\mathrm{o}} < 0 \end{cases}, & \mathbf{x}_0 \notin \mathcal{K} \end{cases} \quad (12)$$

where the first case refers to a situation in which the initial state is part of the critical set of states $\mathcal{K} := \{\mathbf{x} : \kappa(\mathbf{x}) \le \kappa_0\}$.

Secondly, t_{B} is used to calculate $v_{\mathrm{coll,B}}$ from (11b). Inserted into (10), this yields the collision energy reduction:

$$\Delta E = \begin{cases} \begin{cases} a_x^{\mathrm{e}}\,\frac{2x_0}{2a_x^{\mathrm{o}} x_0 - v_{x,0}^2}, & a_x^{\mathrm{o}} - \frac{v_{x,0}^2}{2x_0} \le a_x^{\mathrm{e}} \le 0 \\ 1, & a_x^{\mathrm{e}} \le a_x^{\mathrm{o}} - \frac{v_{x,0}^2}{2x_0} \end{cases}, & \mathbf{x}_0 \in \mathcal{K} \\ \begin{cases} \frac{a_x^{\mathrm{e}}}{\kappa_0}, & \kappa_0 < a_x^{\mathrm{e}} < 0 \\ 1, & a_x^{\mathrm{e}} \le \kappa_0 \end{cases}, & \mathbf{x}_0 \notin \mathcal{K} \end{cases} \quad (13)$$

If the initial state is not already critical (third and fourth case in (13)), the activation timing of the BTN guarantees that the collision will be avoided ($\Delta E = 1$) for a threshold $\kappa_0 = a_x^{\mathrm{e}}$.

Values of ΔE are visualised in Fig. 6a over combinations of the initial state $(x_0, v_{x,0})$ and $\kappa_0 = a_x^{\mathrm{e}}$. The boundary of the plateau, which is described by (2) and has been previously seen in Fig. 3, indicates the region where a collision is already unavoidable for the initial state.

B. Case with uncertainties

In contrast to the deterministic case, the Bayesian activation criterion (9) cannot be analytically solved for t in general. Therefore, the integral is numerically evaluated and solved for the smallest time $t_{\mathrm{B},\mathfrak{U}}$ for which the criterion is fulfilled.

The difference to the deterministic case $\delta t_{\mathrm{B}} := t_{\mathrm{B}} - t_{\mathrm{B},\mathfrak{U}}$ is visualised in Fig. 5 and three distinct effects can be observed:

1) The worst delays occur at the boundary (2) between the critical and uncritical region. In these situations, very limited time is available to increase the confidence before the brake intervention would have been already initiated under ideal conditions.
2) Along this boundary, the results deteriorate for increasing distances. This is due to the distance-dependent accuracy of the stereo vision measurement model (4).
3) Trajectories starting in the area of unavoidable collisions or sufficiently before are less affected by uncertainties. In the first case, (9) is fulfilled almost immediately. In the second case, sufficient time and sensor measurements are available before an intervention is required. Thus, the uncertainty in the state estimate is minimised and small values of the variance $\sigma_\kappa^2(t)$ are ensured.

We remark that the obtained values are often multiple times larger than the assumed system sampling time. This emphasises the relevance of uncertainties in the system.

Although δt_{B} is not available in closed form in general, one can derive analytical expressions for the collision energy

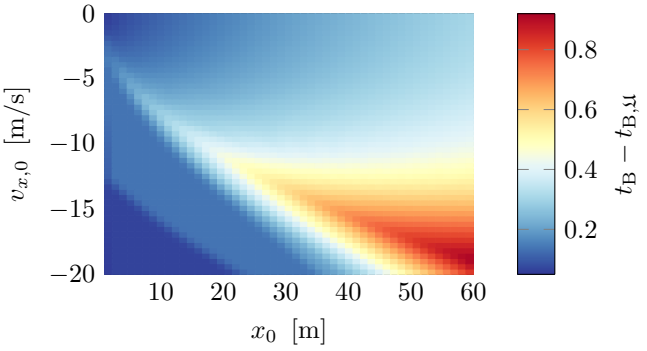

Fig. 5: Difference in braking time $\delta t_\mathrm{B} = t_\mathrm{B} - t_{\mathrm{B},\mathfrak{U}}$ over $(x_0, v_{x,0})$ for $a_x^\mathrm{o} = -3\,\mathrm{m/s^2}$. Positive values indicate that triggering the emergency brake intervention is delayed.

reduction in terms of δt_B. To this end, (10) is calculated for an impact velocity of $v_{\mathrm{coll,B}} + a_x^\mathrm{e}\delta t_\mathrm{B}$:

$$\Delta E_\mathfrak{U} = \Delta E - a_x^\mathrm{e}\frac{\delta t_\mathrm{B}^2 a_x^\mathrm{o} + 2\delta t_\mathrm{B}\left(t_\mathrm{B} a_x^\mathrm{o} + v_{x,0}\right)}{v_{x,0}^2 - 2a_x^\mathrm{o} x_0}\,. \qquad (14)$$

A delay δt_B of an AEB activation reduces the relative collision energy reduction quadratically. Absolute values of $\Delta E_\mathfrak{U}$ are visualised in Fig. 6b.

C. Weighting over scenario distributions

For a meaningful assessment of a system, one has to take into account that not every scenario occurs with the same frequency in real world traffic. Therefore, a weighted average value of the collision energy reduction from Fig. 6 is now calculated using the empirical distributions from Fig. 4.

Furthermore, it has been assumed so far that sensor measurements are available right from the time $t = 0$ of the other vehicle starting to slow down. However, in practice, a sensor's field of view is limited and the first time when an AEB becomes aware of a possibly threatening situation depends on the initial state $(x_0, v_{x,0})$. Therefore, the sensor's longitudinal range of detection $x_{\mathrm{sens,max}}$ is additionally taken into account. This is a best case assumption since other effects which might limit a sensor's field of view, e.g. dynamic occlusions, are not considered.

Taking these effects into account leads to the results that are shown in Fig. 7. Each point is the weighted average of ΔE as previously seen in Fig. 6 over the distribution of $(x_0, v_{x,0})$ from Fig. 4a for one combination of object acceleration a_x^o and sensor range $x_{\mathrm{sens,max}}$. As is expected, increasing the sensor range has a positive effect. We note that even in the baseline case without uncertainties, perfect results cannot be achieved, especially for high absolute values of a_x^o. As has been seen in Fig. 6a, a collision is never avoidable for certain combinations of low initial distance and high relative velocity, due to the limited braking capabilities. Nevertheless, the weighted average in Fig. 7a reaches values close to one for $a_x^\mathrm{o} \geq -6\,\mathrm{m/s^2}$. This indicates that human drivers avoid combinations of distance and relative velocity that are very sensitive to an unexpected braking of a preceding vehicle.

If these results are furthermore weighted with the empirical distribution of a_x^o from Fig. 4b, one obtains the results shown in Fig. 8. With uncertainties taken into account, the average effectiveness drops by approximately 20%. Thus, although an optimistic model with lower bounds on the state estimation uncertainty is employed, the effect on the eventual performance of the AEB system is not neglectable.

V. Conclusion

This work has analysed the influence of uncertainties on the collision prevention capabilities of an AEB system. The analysis is founded on analytical uncertainty propagation in algorithms for perception, state estimation and criticality assessment. Results from a numerical example demonstrate the concrete application of the method.

It is found that uncertainties affect the system's ability to perform a timely emergency brake activation depending on the driving scenario. The worst delays are obtained in scenarios which start close to an unavoidable collision and thus leave only little time for plausibilisation. Fortunately, such situations are not predominant in real world traffic, as has been seen from empirical scenario distributions. Therefore, the weighted average results show a high collision avoidance benefit.

In order to derive the probabilistic model, uncertainties in sensor measurements are propagated to the state estimation and criticality assessment layers. Finally, the time, at which a brake intervention can be initiated with sufficient confidence, is calculated. Future works could attempt to derive this timing in a more abstract way, e.g. in a hypothesis testing framework as discussed in [15], [16]. Moreover, following the framework proposed in [4], one could investigate the statistical properties of ΔE in order to derive performance requirements for sensors and estimation algorithms analogous to (9).

Finally, AEB systems are only one cornerstone on the way to highly automated driving. Therefore, future works should address models of more sophisticated algorithms.

References

[1] J. Nilsson, A. Ödblom, and J. Fredriksson, "Worst case analysis of automotive collision avoidance systems," *Vehicular Technology, IEEE Transactions on*, vol. 65, no. 4, pp. 1899–1911, 2016.

[2] J. E. Stellet, J. Schumacher, O. Lange, W. Branz, F. Niewels, and J. M. Zöllner, "Statistical modelling of object detection in stereo vision-based driver assistance," in *Intelligent Autonomous Systems 13*, ser. Advances in Intelligent Systems and Computing, 2016, vol. 302, pp. 749–761.

[3] J. E. Stellet, F. Straub, J. Schumacher, W. Branz, and J. M. Zöllner, "Estimating the process noise variance for vehicle motion models," in *Intelligent Transportation Systems (ITSC), 18th IEEE International Conference on*, 2015, pp. 1512–1519.

[4] J. E. Stellet, J. Schumacher, W. Branz, and J. M. Zöllner, "Uncertainty propagation in criticality measures for driver assistance," in *Intelligent Vehicles Symposium (IV), IEEE*, 2015, pp. 1187–1194.

[5] T. Maurer, "Bewertung von Mess- und Prädiktionsunsicherheiten in der zeitlichen Eingriffsentscheidung für automatische Notbrems- und ausweichsysteme," Ph.D. thesis, Universität Duisburg-Essen, 2013.

[6] C. Braeuchle, F. Flehmig, W. Rosenstiel, and T. Kropf, "Maneuver decision for active pedestrian protection under uncertainty," in *Intelligent Transportation Systems (ITSC), 16th IEEE International Conference on*, 2013, pp. 646–651.

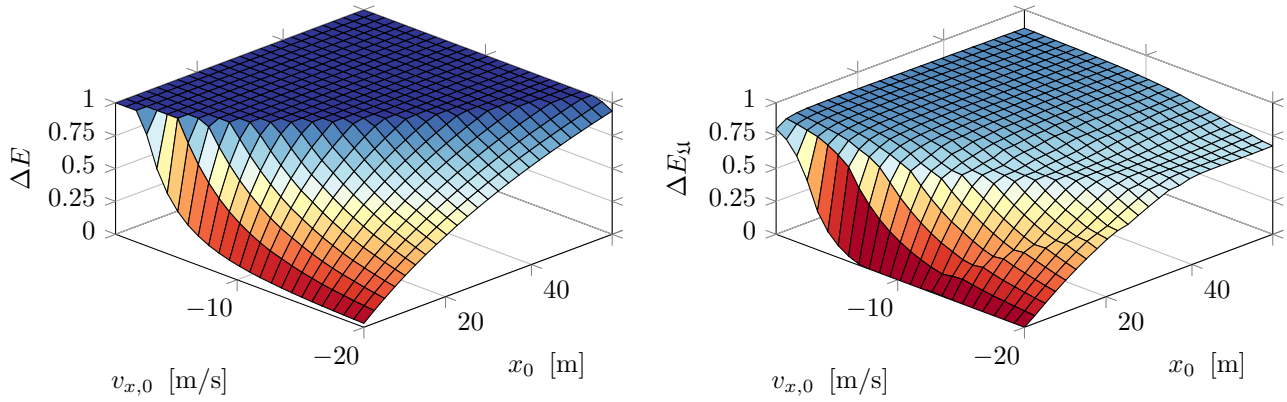

(a) Deterministic baseline case.

(b) Under uncertainty.

Fig. 6: Relative reduction of the collision energy by AEB brake intervention over $(x_0, v_{x,0})$ for $a_x^{\mathrm{o}} = -3\,\mathrm{m/s^2}$. The baseline case of with ideal knowledge of the state is shown in (a). Results under the influence of uncertainties are visualised in (b).

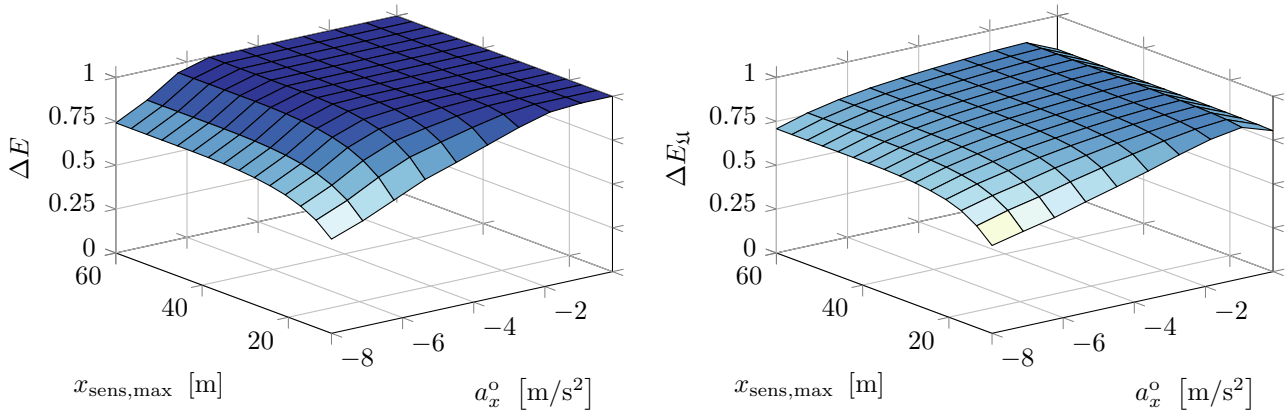

(a) Deterministic baseline case.

(b) Under uncertainty.

Fig. 7: Relative reduction of the collision energy from Fig. 6 weighted with the distribution of the scenario parameters $(x_0, v_{x,0})$ from Fig. 4a. The weighted means are shown over combinations of $x_{\mathrm{sens,max}}$ and a_x^{o}.

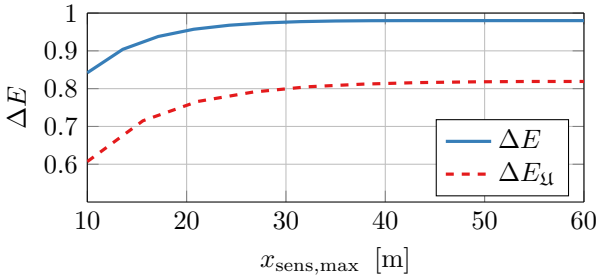

Fig. 8: The results from Fig. 7 are weighted with the empirical distribution of a_x^{o} from Fig. 4b. This graph shows the relation between the effectiveness of an AEB and the sensor detection range $x_{\mathrm{sens,max}}$.

[7] P. Themann, J. Kotte, D. Raudszus, and L. Eckstein, "Impact of positioning uncertainty of vulnerable road users on risk minimization in collision avoidance systems," in *Intelligent Vehicles Symposium (IV), IEEE*, 2015, pp. 1201–1206.

[8] J. Hoffmann, "Das Darmstädter Verfahren (EVITA) zum Testen und Bewerten von Frontalkollisionsgegenmaßnahmen," Ph.D. thesis, Technische Universität Darmstadt, 2008.

[9] H. Badino, "Binocular ego-motion estimation for automotive applications," Ph.D. thesis, Goethe Universität Frankfurt am Main, 2008.

[10] P. Tichavsky, C. Muravchik, and A. Nehorai, "Posterior cramer-Rao bounds for discrete-time nonlinear filtering," *Signal Processing, IEEE Transactions on*, vol. 46, no. 5, pp. 1386–1396, 1998.

[11] G. Hendeby, "Performance and implementation aspects of nonlinear filtering," Ph.D. thesis, Linköping University, 2008.

[12] J. Jansson, "Collision avoidance theory : with application to automotive collision mitigation," Ph.D. thesis, Linköping University, 2005.

[13] M. Schreier, V. Willert, and J. Adamy, "Bayesian, maneuver-based, long-term trajectory prediction and criticality assessment for driver assistance systems," in *Intelligent Transportation Systems (ITSC), 17th IEEE International Conference on*, 2014, pp. 334–341.

[14] N. Kaempchen, B. Schiele, and K. Dietmayer, "Situation assessment of an autonomous emergency brake for arbitrary vehicle-to-vehicle collision scenarios," *Intelligent Transportation Systems, IEEE Transactions on*, vol. 10, no. 4, pp. 678–687, 2009.

[15] S. Lefevre, R. Bajcsy, and C. Laugier, "Probabilistic decision making for collision avoidance systems: Postponing decisions," in *Intelligent Robots and Systems (IROS), IEEE/RSJ International Conference on*, 2013, pp. 4370–4375.

[16] J. E. Stellet, J. Schumacher, W. Branz, and J. M. Zöllner, "Performance bounds on change detection with application to manoeuvre recognition for advanced driver assistance systems," in *Intelligent Vehicles Symposium (IV), IEEE*, 2015, pp. 1112–1119.